



**HAL**  
open science

## Dissipation in unsteady turbulence

Wouter J.T. Bos, Robert Rubinstein

► **To cite this version:**

Wouter J.T. Bos, Robert Rubinstein. Dissipation in unsteady turbulence. *Physical Review Fluids*, 2017, 10.1103/PhysRevFluids.2.022601 . hal-01380627v2

**HAL Id: hal-01380627**

**<https://hal.science/hal-01380627v2>**

Submitted on 13 Oct 2022

**HAL** is a multi-disciplinary open access archive for the deposit and dissemination of scientific research documents, whether they are published or not. The documents may come from teaching and research institutions in France or abroad, or from public or private research centers.

L'archive ouverte pluridisciplinaire **HAL**, est destinée au dépôt et à la diffusion de documents scientifiques de niveau recherche, publiés ou non, émanant des établissements d'enseignement et de recherche français ou étrangers, des laboratoires publics ou privés.

# Dissipation in unsteady turbulence

Wouter J.T. Bos<sup>1</sup> and Robert Rubinstein<sup>2</sup>

<sup>1</sup> LMFA, CNRS, Ecole Centrale de Lyon - Université de Lyon - Ecullly, France

<sup>2</sup> Newport News, VA, USA

Recent experiments and simulations have shown that unsteady turbulent flows display a universal behaviour at short and intermediate times, different from classical scaling relations. The origin of these observations is explained using a non-equilibrium correction to Kolmogorov's energy spectrum, and the exact form of the observed, universal scaling is derived.

## I. INTRODUCTION

Taylor's dissipation rate estimate [1], and Kolmogorov's inertial range scaling [2] are corner-stones of the description of turbulent flows. In recent experiments [3] it was observed that in a number of situations where Taylor's estimate is not valid, another universal expression fits the data, depending both on the local flow features and the initial conditions. In this manuscript we will show that these observations can be explained using an unsteady correction to Kolmogorov's inertial range spectrum.

Kolmogorov's concepts, introduced in the 1940s, state that the energy distribution among scales at sufficiently high Reynolds number is completely determined by the scale-size and the energy flux through scales, for scale-sizes sufficiently small compared to the most energetic eddies, and sufficiently large compared to the smallest, dissipative scales. In this range the energy spectrum is approximately given by the relation,

$$E(\kappa, t) = C_K \epsilon(t)^{2/3} \kappa^{-5/3}, \quad (1)$$

where  $\epsilon(t)$  is the average dissipation rate,  $\kappa$  the wavenumber, and  $C_K \approx 1.5$  a constant. This relation is observed, to a good approximation, in a wide range of turbulent flows. Taylor's dissipation rate estimate,

$$\epsilon(t) = C_\epsilon \frac{U(t)^3}{L(t)}, \quad (2)$$

relates the dissipation rate, which is in principle a small scale quantity, to the dynamics of the large-scale quantities  $U$ , the RMS velocity and  $L$  the integral lengthscale [4, 5]. The insight that the dissipation can be modeled using large-scale quantities, allows the formulation of simple engineering models that need not take into account the multi-scale character of turbulence. Both relations are intimately related [6, 7] and an estimate of the constant  $C_\epsilon$  can be obtained using relation (1) (details are given below). The quantity  $C_\epsilon$  can be expressed as a function of two distinct Reynolds numbers, through the relation,

$$C_\epsilon \sim \frac{R_L(t)}{R_\lambda(t)^2} \quad (3)$$

where

$$R_L(t) = \frac{U(t)L(t)}{\nu}, \quad R_\lambda(t) = \sqrt{15 \frac{U(t)^4}{\nu \epsilon(t)}}, \quad (4)$$

where it can be noted that  $C_\epsilon$  is independent of the viscosity  $\nu$ .

Recent experimental studies at Imperial College London, considering decaying wind-tunnel turbulence behind different types of turbulence-generating grids [8–11], have focused on both the regions of the flow near the grid, and farther away from it. Their results seem to show that far away from the grid, if the initial Reynolds number is large enough, the classic result (2) is obtained. However, in an adjacent region, closer to the grid, another seemingly universal law is observed,

$$C_\epsilon \sim \frac{\sqrt{R_L(0)}}{R_\lambda(t)} \quad (5)$$

where  $R_L(0)$  is determined by the initial conditions. Other research groups confirmed the results in independent grid-turbulence experiments [12–14] and direct numerical simulations [15]. The scaling observed in these experiments seems more general than the case of freely decaying grid-turbulence only, since experiments and simulations of the wakes generated by plates with both regular and irregular edges show the same tendency [16–18]. Recently, it was shown that in yet another different type of turbulent flow, where the kinetic energy is maintained at a certain level through an external forcing, the fluctuations of kinetic energy and dissipation around the long-time-averaged state can be described by the same law [19].

It is noted that expression (5) is radically different from (3), since expression (5) depends on the initial conditions and the local flow properties, whereas (3) only involves local quantities. Since, as stated before,  $C_\epsilon$  can be related to Kolmogorov's energy spectrum (1), (5) might suggest a departure from (1) during the transient, but this is not observed. Our analysis explains these puzzling results. In particular it is shown that the observation of (5) is related to a sub-dominant correction to Kolmogorov's energy spectrum first proposed in [20]. In the next section we reproduce a simple derivation of this non-equilibrium correction. In section III, the correction to the dissipation rate estimate is determined. In section

IV, the derived relations are compared to existing experimental and numerical results. Section V concludes this paper.

## II. DERIVATION OF THE NON-EQUILIBRIUM ENERGY SPECTRUM

We reproduce here the simplest possible derivation of the non-equilibrium correction to the energy spectrum. The same results were obtained by [21, 22] using similarity arguments, using Kovaznay's closure in [23] and using more sophisticated closures in [20, 24].

We start from the evolution equation for the kinetic energy spectrum at high Reynolds numbers at scales where both production and dissipation mechanisms can be neglected,

$$\partial_t E(\kappa, t) = -\partial_\kappa \Pi(\kappa, t), \quad (6)$$

where  $\Pi(\kappa, t)$  is a flux of energy which should vanish at  $\kappa = 0$  and  $\kappa = \infty$ . This relation states that in a steady state, where the LHS vanishes, in the inertial range, the flux is conserved (and thus independent of  $\kappa$ ), so that the RHS also vanishes.

We make the assumption that we can decompose the energy spectrum into its *equilibrium* and *non-equilibrium* parts,

$$E(\kappa, t) = \bar{E}(\kappa, t) + \tilde{E}(\kappa, t). \quad (7)$$

It is extremely important for the following to note that both parts are a function of time and that this is not a separation of the energy distribution in a steady and an unsteady part. The determination of the equilibrium part of the flow will be discussed in section IV A. For the moment we will content ourselves by defining the equilibrium part of the turbulence as the part for which the flux is not a function of scale  $\bar{\Pi}(\kappa, t) = \epsilon(t)$  and therefore  $\partial_\kappa(\bar{\Pi} + \tilde{\Pi}) = \partial_\kappa \tilde{\Pi}$ , yielding for the evolution of the spectrum,

$$\partial_t \bar{E}(\kappa, t) = -\partial_\kappa \tilde{\Pi}(\kappa, t), \quad (8)$$

where we focus on the analytically tractable case of small nonequilibrium,  $|\partial_t \tilde{E}(\kappa, t)| \ll |\partial_t \bar{E}(\kappa, t)|$ . It is at this point that we need the introduction of an assumption on the functional form of the flux. In the present derivation, we consider Kovaznay's model [25] for the flux,

$$\Pi(\kappa, t) = C_K^{-3/2} \kappa^{5/2} E(\kappa, t)^{3/2}. \quad (9)$$

The choice of this model will limit our considerations to the inertial-range interval of the energy distribution. More complicated closures would be needed to take into account a realistic infrared range for small  $\kappa$ , or more complex situations where anisotropy or inhomogeneity are present. Expression (9) immediately yields, when  $\Pi(\kappa, t) = \epsilon(t)$ , that  $\bar{E}(\kappa, t)$  is given by,

$$\bar{E}(\kappa, t) = C_K \epsilon(t)^{2/3} \kappa^{-5/3}. \quad (10)$$

Introducing (7) into (9) yields for small perturbations,

$$\begin{aligned} \Pi(\kappa, t) &= C_K^{-3/2} \kappa^{5/2} \bar{E}(\kappa, t)^{3/2} \left( 1 + \frac{3 \tilde{E}(\kappa, t)}{2 \bar{E}(\kappa, t)} \right), \\ &= \epsilon(t) \left( 1 + \frac{3 \tilde{E}(\kappa, t)}{2 \bar{E}(\kappa, t)} \right). \end{aligned} \quad (11)$$

Substituting this into expression (8) gives upon integration

$$\tilde{E}(\kappa, t) = C_K \Omega_\epsilon(t) \epsilon(t)^{1/3} \kappa^{-7/3}, \quad (12)$$

with

$$\Omega_\epsilon(t) = \frac{2C_K}{3} \frac{\dot{\epsilon}(t)}{\epsilon(t)}. \quad (13)$$

It is this new frequency  $\Omega_\epsilon$  in the dynamics which allows to find the  $\kappa^{-7/3}$  scaling in (12) as a first linear correction to classical scaling, as for the shear-stress spectrum in homogeneous shearflow, where the mean-velocity gradient is introduced as typical frequency [26]. The small parameter in our derivation is  $\tilde{E}(\kappa, t)/\bar{E}(\kappa, t)$ . Combining the Kolmogorov scaling with (12), one finds that

$$\frac{\tilde{E}(\kappa, t)}{\bar{E}(\kappa, t)} = \Omega_\epsilon(t) \epsilon(t)^{-1/3} \kappa^{-2/3}, \quad (14)$$

showing that the validity of the approximation should improve as the wavenumber increases.

Both spectra (10) and (12) are a function of time. The equilibrium part describes thus not necessarily a steady state, and temporal fluctuations are therefore not purely described by (12), since if they are slow enough, they will have time to adapt to the equilibrium distribution (10). The observation of the non-equilibrium scaling (12) is not straightforward, since it is subdominant with respect to the Kolmogorov spectrum (10). Conditional averaging allows however to extract the unsteady energy spectrum, as was illustrated in reference [23], where a clear  $\kappa^{-7/3}$  wavenumber spectrum was observed in a statistically steady turbulent flow simulation. The difference in wavenumber scaling between  $\bar{E}(\kappa, t)$  and  $\tilde{E}(\kappa, t)$  is the origin of the observations of a non-classical, but universal transient scaling of the dissipation rate. We will elaborate on that in the following. We note that the possible relevance of the spectrum suggested by Yoshizawa (12) to estimate the dissipation rate in unsteady turbulence was already mentioned in reference [27].

## III. DERIVATION OF THE NEW DISSIPATION SCALING

To simplify the considerations we assume the two scalings (10) and (12) to hold in the wavenumber interval

between  $\kappa_0$ , the forcing scale and  $\kappa_\eta$ , the Kolmogorov scale, given by

$$\kappa_\eta \sim \frac{\bar{\epsilon}(t)^{1/4}}{\nu^{3/4}}. \quad (15)$$

Outside this interval the kinetic energy is assumed to be zero, for analytical convenience. We have also considered more complicated spectra adding a more realistic infrared energy range (as in [7]) and the results hereafter were shown to be robust. All quantities will be decomposed into their equilibrium part, indicated by a bar and their non-equilibrium part, indicated by a tilde. For instance  $C_\epsilon = \bar{C}_\epsilon + \tilde{C}_\epsilon$ ,  $\epsilon = \bar{\epsilon} + \tilde{\epsilon}$ , etc. The equilibrium kinetic energy is computed by integrating expression (10),

$$\bar{k}(t) = \int \bar{E}(\kappa, t) d\kappa = (3/2)\bar{U}(t)^2, \quad (16)$$

and, similarly the non-equilibrium energy is obtained from equation (12). The integral lengthscale is defined by

$$L(t) = \frac{3\pi}{4} \frac{\int \kappa^{-1} E(\kappa, t) d\kappa}{\int E(\kappa, t) d\kappa} \equiv \frac{3\pi}{4} \frac{\mathcal{I}(t)}{k(t)}. \quad (17)$$

where we introduced  $\mathcal{I}(t) \equiv \int \kappa^{-1} E(\kappa, t) d\kappa$  for later convenience. The dissipation can be computed from the energy spectrum by

$$\epsilon(t) = 2\nu \int \kappa^2 E(\kappa, t) d\kappa, \quad (18)$$

where all integrals are evaluated on the interval  $[\kappa_0, \kappa_\eta]$ . Carrying out these integrals using (10) to evaluate  $\bar{U}$  and  $\bar{L}$  (expressions (16) and (17)), and substituting these expressions in Kolmogorov's and Taylor's expressions (1) and (2), it is immediately found that the equilibrium value of the normalized dissipation rate is

$$\bar{C}_\epsilon = \frac{3\pi}{10} C_K^{-3/2} \approx 0.51. \quad (19)$$

This value is thus the inertial range estimate of  $C_\epsilon$ , assuming a spectrum given by (1) on the interval  $[\kappa_0, \kappa_\eta]$ . Despite such gross assumptions on the shape of the energy spectrum, its value is actually close to the value observed in direct numerical simulations of forced high Reynolds numbers turbulence where values around 0.5 are observed [5]. In the following we will omit the time-dependence of the different quantities to lighten the notation. It should however be kept in mind, as we stressed before, that both the equilibrium and the non-equilibrium quantities can depend on time.

Since  $C_\epsilon \sim \epsilon \mathcal{I} / k^{5/2}$ , we can write without any approximations

$$\frac{C_\epsilon}{\bar{C}_\epsilon} = \frac{(1 + \frac{\tilde{\epsilon}}{\bar{\epsilon}}) \left(1 + \frac{\tilde{\mathcal{I}}}{\bar{\mathcal{I}}}\right)}{\left(1 + \frac{\tilde{k}}{\bar{k}}\right)^{5/2}}. \quad (20)$$

The different quantities in this expression are obtained by integrating the expressions (16), (17) and (18) over the interval  $[\kappa_0, \kappa_\eta]$ , using the spectra (10) and (12) for the equilibrium and nonequilibrium contributions, respectively. For instance, it is found that

$$\frac{\tilde{\epsilon}}{\bar{\epsilon}} = \frac{2\Omega_\epsilon}{\epsilon^{1/3} \kappa_\eta^{2/3}} \quad \text{and} \quad \frac{\tilde{k}}{\bar{k}} = \frac{\Omega_\epsilon}{2\epsilon^{1/3} \kappa_0^{2/3}}, \quad (21)$$

where we have assumed  $\kappa_0 \ll \kappa_\eta$ . Since in the equilibrium state  $\kappa_0/\kappa_\eta \sim R_\lambda^{-3/2}$ , we find that

$$\frac{\tilde{\epsilon}}{\bar{\epsilon}} \sim R_\lambda^{-1} \frac{\tilde{k}}{\bar{k}}, \quad (22)$$

which is a direct consequence of the  $k^{-7/3}$  scaling of  $\tilde{E}(k)$ . This shows that the  $\tilde{\epsilon}/\bar{\epsilon}$  term in (20) is negligible. This indicates also that the temporal dissipation rate fluctuations observed in [19, 27] are mainly related to the equilibrium distribution  $\bar{E}(k, t)$  of the flow and negligibly contribute to the non-equilibrium part of the dissipation rate. We further find that  $\tilde{\mathcal{I}}/\bar{\mathcal{I}} = (10/7)\tilde{k}/\bar{k}$ . The expression for large Reynolds numbers is therefore

$$\frac{C_\epsilon}{\bar{C}_\epsilon} \approx \frac{\left(1 + \frac{10}{7} \frac{\tilde{k}}{\bar{k}}\right)}{\left(1 + \frac{\tilde{k}}{\bar{k}}\right)^{5/2}}. \quad (23)$$

Evaluating the Reynolds number one finds analogously,

$$\frac{R_\lambda}{\bar{R}_\lambda} \approx \left(1 + \frac{\tilde{k}}{\bar{k}}\right). \quad (24)$$

where  $\bar{R}_\lambda$  is given by (4) using the equilibrium values  $\bar{U}$  and  $\bar{\epsilon}$ . To obtain these two expressions we have thus only assumed that the Reynolds number is high and that the energy spectrum can be represented by (10) and (12) between  $\kappa_0$  and  $\kappa_\eta$ . We consider the case where  $\tilde{k}/\bar{k}$  is small, for which the non-equilibrium scaling (12) was derived, so that we can use a Taylor-expansion to rewrite (23) as

$$\frac{C_\epsilon}{\bar{C}_\epsilon} \approx \left(1 + \frac{\tilde{k}}{\bar{k}}\right)^{-15/14} = \left(\frac{R_\lambda}{\bar{R}_\lambda}\right)^{-15/14}. \quad (25)$$

and this is our prediction for the Reynolds number dependence of the normalized dissipation rate. To appreciate the similarity with the experimentally observed powerlaw (5) one needs to realize that  $\sqrt{R_L(0)} \sim \bar{R}_\lambda$  (combining expressions (2) and (4)) and that  $\bar{C}_\epsilon$  is a constant, so that this expression can be rewritten as

$$C_\epsilon \sim \left(\frac{\sqrt{R_L(0)}}{R_\lambda(t)}\right)^{15/14}, \quad (26)$$

and we find to a good approximation expression (5). Indeed, the difference between (5) and (26) will in most

cases be small enough to fall into experimental error-bars or the convergence of statistical averages in simulations. We further mention here also that in the experimental and numerical investigations reported in [3] the possibility was left open that the exponents are not exactly, but only close to the ones in expression (5).

#### IV. COMPARISON WITH EXISTING RESULTS

##### A. Determining the equilibrium state

At this point we will compare to existing results from literature. A subtle point is how one can identify the equilibrium part of a flow. The quantities that we need to determine first are the equilibrium values  $\bar{U}$ ,  $\bar{L}$  and  $\bar{\epsilon}$ . We have considered here isotropic turbulence. For such flows the equilibrium state is the Kolmogorov constant flux state, where

$$\bar{\Pi}(\kappa, t) = \epsilon(t). \quad (27)$$

Such a state needs an energy input at large-scales which is in equilibrium with the dissipation  $\epsilon(t)$  at small scales. Probably the best approximation of a constant flux state can be obtained in Direct Numerical Simulations with an external forcing term. In practice, due to the finite size of the simulated domain, fluctuations of the energy input and the dissipation rate will always lead to a certain amount of imbalance. The time-average of the energy-injection will however balance the time-averaged energy dissipation, so that for such flows the equilibrium values of  $\bar{U}$ ,  $\bar{L}$  and  $\bar{\epsilon}$  are obtained by time-averaging.

The comparison of our prediction with existing experimental results on grid-generated turbulence in a wind-tunnel is not straightforward since in the vicinity of the grid the turbulence is not statistically homogeneous, nor isotropic. It is in this production zone where the kinetic energy is injected into the flow by the shear layers generated by the wakes of the grid-bars. The constant flux state, where the dissipation is in equilibrium with the production, corresponds to the point in the flow where the kinetic energy attains its maximum. At short distances beyond this point the equilibrium spectrum can be considered constant in time, compared to the non-equilibrium part. For larger times the equilibrium spectrum will evolve. We do not have access to experimental results for the equilibrium energy distribution at later times and we will therefore use the flow at the energy peak to estimate the equilibrium values of the different quantities in our comparison with experiment.

##### B. The dissipation scaling

As mentioned above, for a forced DNS in a statistically steady state the equilibrium is straightforwardly identified by time-averaging. Furthermore in a periodic domain, an instantaneous space average will tend to the

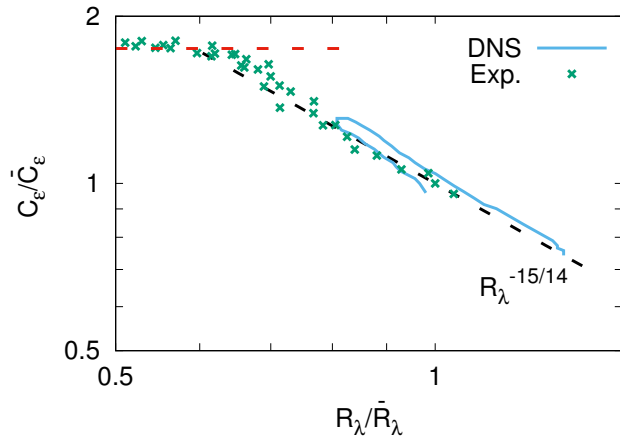


FIG. 1. The prediction of the normalized dissipation rate as a function of the Reynolds number ratio  $R_\lambda/\bar{R}_\lambda$ , expressions (25) and (29), compared to numerical [19] and experimental [10] results.

same, ensemble average, if the volume over which is averaged contains a sufficient number of flow structures. In practice this is never the case and temporal fluctuations will be observed around a long-time averaged flow [19]. These box-averaged fluctuations are not necessarily in equilibrium and will thereby give rise to an evolution of  $C_\epsilon$ . We have plotted in Figure 1 the results of reference [19] Figure 3, for the fluctuations of  $C_\epsilon$  around its average value for their highest Reynolds number ( $700 < R_\lambda < 1000$ ) as a function of the ratio of the Reynolds number to its time-averaged value which we call  $\bar{R}_\lambda$ . It is observed that those results are in perfect agreement with our prediction.

We have also attempted a comparison with the experimental results reported in [10]. We have replotted in Fig. 1 the data from their Fig. 6, where the Reynolds number varies in the range  $290 > R_\lambda > 111$ . As argued above, we have considered their first data-point, corresponding to the peak-value of the kinetic energy, as the equilibrium state determining  $\bar{R}_\lambda$ . At this point a value of  $C_\epsilon \approx 0.5$  is found for the equilibrium value of the normalized dissipation rate. It is observed that the experimental results, like the simulation, reproduce the theoretical prediction (25) exactly.

At this point, an open question is whether our analysis is relevant for decaying turbulence at long times, where  $C_\epsilon$  settles to a constant value, different from its equilibrium value. We will consider the case where the kinetic energy decays following a powerlaw  $k = k_0(t/t_0)^{-n}$ . The precise values of the reference quantities  $k_0$  and  $t_0$  are not important in the following. Deriving this expression for  $k$  twice to obtain expressions for  $\epsilon$  and  $\dot{\epsilon}$  gives  $\dot{\epsilon}/\epsilon = -(n+1)/t$  and  $\epsilon/k = n/t$ . Using these relations, integrating equations (10) and (12) and eliminating  $\kappa_0$

from the expressions, it is immediately found that

$$\frac{\tilde{k}}{\bar{k}} = -\frac{2n+1}{9n}, \quad (28)$$

and therefore, we find for the dissipation rate constant using (25),

$$\frac{C_\epsilon}{\bar{C}_\epsilon} \approx \left( \frac{9n}{7n-2} \right)^{15/14}. \quad (29)$$

The value of  $n$  is in general contained in the range  $1 \leq n \leq 2$ , leading to the ratio  $1.8 \geq C_\epsilon/\bar{C}_\epsilon \geq 1.54$ , which is a rather realistic range of values when compared to experiments and simulations [7]. In Fig. 1 we have added the asymptotic value  $C_\epsilon/\bar{C}_\epsilon = 1.75$  corresponding to a decay-exponent  $n = 1.2$ , typical for decaying grid-generated turbulence, which fits the long-time data accurately. Self-similar decay is therefore, in our framework, not an equilibrium, but a state where the disequilibrium is a constant fraction of the total kinetic energy,  $\tilde{k}(t)/\bar{k}(t) \neq f(t)$ .

These ideas explain why in the experimental and numerical results in [3] the Reynolds number decays before Taylor's expression is observed. Indeed, the imbalance is not a low-Reynolds number effect and in the experiments and simulations the Reynolds number is in principle high enough to observe both Taylor's and Kolmogorov's scaling. However, the evolution of both  $R_\lambda$  and  $C_\epsilon$  is a function of  $\tilde{k}/\bar{k}$ . In turbulent flows in which the kinetic energy at long times decays following a power law, this latter quantity evolves from zero to a constant value, given by expression (28). The Reynolds number decays thus during the non-equilibrium transient from its initial value to a value

$$\frac{R_\lambda}{\bar{R}_\lambda} \approx \frac{7n-2}{9n}. \quad (30)$$

When this phase is attained and both  $R_\lambda$  and  $\bar{R}_\lambda$  decay following power laws, this ratio remains constant.

### C. Time evolution of turbulent lengthscales

Following the above arguments, we can also predict how the ratio of the integral to Taylor lengthscales evolves during the non-equilibrium phase. The Taylor scale is given by

$$\lambda = \sqrt{\frac{10\nu k}{\epsilon}}. \quad (31)$$

Combining this relation with the definition (17) for  $L$ , we find using the same arguments as for  $C_\epsilon$ , that

$$\frac{\lambda/L}{\bar{\lambda}/\bar{L}} = \left( \frac{R_\lambda}{\bar{R}_\lambda} \right)^{1/14}. \quad (32)$$

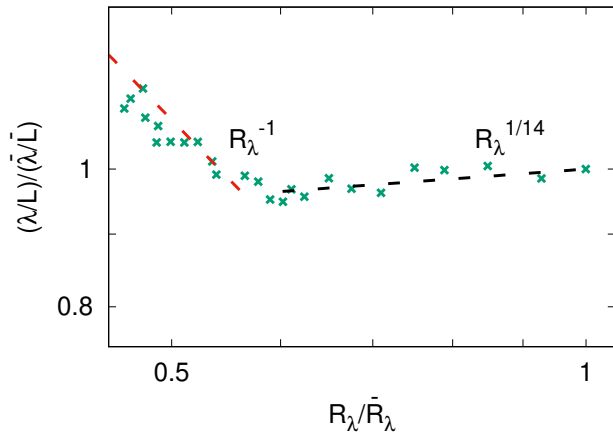


FIG. 2. The prediction of the ratio of the Taylor-scale to the integral scale on the Reynolds number ratio  $R_\lambda/\bar{R}_\lambda$ , compared to experimental results [10]. Also shown is a comparison to the classical Reynolds number dependence of  $\lambda/L$ , Eq. (33).

This small value of the exponent explains why it was observed that the lengthscales ratio in the experiments remained approximately constant in the region of the flows where the non-equilibrium scaling was observed. In Figure 2 it is observed that this powerlaw accurately describes the data.

When the Reynolds number drops to the value corresponding to expression (30), one should retrieve the classical Reynolds number dependence. In this regime, the ratio  $R_\lambda/\bar{R}_\lambda$  remains constant, and the experimental data corresponds then to  $[\lambda(t)/L(t)]/[\lambda(t=0)/L(t=0)]$  as a function of  $R_\lambda(t)/R_\lambda(t=0)$ , where  $t=0$  corresponds to the first (most upstream) data-point. The data should then exhibit the scaling,

$$\frac{\lambda}{L} \sim R_\lambda^{-1}. \quad (33)$$

## V. CONCLUSION

We have presented a simple framework which allows to interpret the non-equilibrium scaling observed in practically all the experiments and simulations mentioned in [3]. The present analysis is important for the modeling and understanding of turbulent flows since the non-equilibrium transient can be long and in many situations a self-similar decay might not even be reached before the flow is perturbed by the influence of boundaries, or because the Reynolds number has decayed too much for (1) and (2) to be valid. Given the agreement with experiments and simulations, the analytical results from the present investigation suggest that the normalized dissipation in a wide class of unsteady turbulent flows can be described by the same, fairly simple, relations.

Expression (25) constitutes the main result of the present work. However, it is not the exact value of the exponent, which is close to the experimental observations, that is of interest. Indeed, its precise value can change slightly as a function of the detailed shape of the energy spectrum. We have checked this by assuming more realistic shapes for the energy containing range, and the results are robust, but the powerlaw exponent can somewhat change. What is of greater importance is that the foregoing analysis gives a firm theoretical basis for the transient behaviour of turbulent flows. The only non-trivial ingredient in the derivation is the shape of the unsteady energy-spectrum  $E(\kappa, t)$  (expression (12)). The present analysis complements thereby recent investigations suggesting that spectral imbalance [27, 28] and large scale coherence [29] are behind the universal scaling of  $C_\epsilon$  in non-equilibrium turbulence.

Since this, rather simple, framework for unsteady turbulence allows to explain practically all the experimental observations in the transient, unsteady phase of devel-

oping turbulent flows [3], it is plausible that engineering models can be improved by taking these ideas into account. We further think that the understanding of more complicated flows can greatly benefit from the insights obtained in this letter. For this to be successful, the ideas, here developed for isotropic turbulence, should be extended to other configurations such as shearflows and turbulent boundary layers. Defining an equilibrium flow for anisotropic and inhomogeneous flows is more delicate, but since the non-equilibrium scaling for the dissipation also describes the turbulent wakes of plates [16–18], we think that at least part of the present ideas can be transposed to more complicated flows.

## VI. ACKNOWLEDGMENTS

The authors have benefited from discussion with J.C. Vassilicos.

- 
- [1] G.I. Taylor. Statistical theory of turbulence. *Proc. Roy. Soc. London. Ser. A, Math. Phys. Sci.*, 151:421–444, 1935.
  - [2] A. N. Kolmogorov. The local structure of turbulence in incompressible viscous fluid for very large Reynolds numbers. *Dokl. Akad. Nauk. SSSR*, 30:301, 1941.
  - [3] J.C. Vassilicos. Dissipation in turbulent flows. *Ann. Rev. Fluid Mech.*, 47:95–114, 2015.
  - [4] K.R. Sreenivasan. On the scaling of the turbulence energy dissipation rate. *Phys. Fluids*, 27:1048, 1984.
  - [5] Y. Kaneda, T. Ishihara, M. Yokokawa, K. Itakura, and A. Uno. Energy dissipation rate and energy spectrum in high resolution direct numerical simulations of turbulence in a periodic box. *Phys. Fluids*, 15(L21), 2003.
  - [6] J.L. Lumley. Some comments on turbulence. *Phys. Fluids*, 4:206, 1992.
  - [7] W. J. T. Bos, L. Shao, and J.-P. Bertoglio. Spectral imbalance and the normalized dissipation rate of turbulence. *Phys. Fluids*, 19:045101, 2007.
  - [8] R.E. Seoud and J.C. Vassilicos. Dissipation and decay of fractal-generated turbulence. *Phys. Fluids*, 19(10):105108, 2007.
  - [9] N. Mazellier and J.C. Vassilicos. Turbulence without richardson–kolmogorov cascade. *Phys. Fluids*, 22(7):075101, 2010.
  - [10] P.C. Valente and J.C. Vassilicos. Universal dissipation scaling for nonequilibrium turbulence. *Phys. Rev. Lett.*, 108(21):214503, 2012.
  - [11] P.C. Valente and J.C. Vassilicos. The non-equilibrium region of grid-generated decaying turbulence. *J. Fluid Mech.*, 744:5–37, 2014.
  - [12] S. Discetti, I. B. Ziskin, T. Astarita, R.J. Adrian, and K. P. Prestridge. Piv measurements of anisotropy and inhomogeneity in decaying fractal generated turbulence. *Fluid Dyn. Res.*, 45(6):061401, 2013.
  - [13] R. J. Hearst and P. Lavoie. Decay of turbulence generated by a square-fractal-element grid. *J. Fluid Mech.*, 741:567–584, 2014.
  - [14] J. C. Isaza, R. Salazar, and Z. Warhaft. On grid-generated turbulence in the near-and far field regions. *J. Fluid Mech.*, 753:402–426, 2014.
  - [15] K. Nagata, Y. Sakai, T. Inaba, H. Suzuki, O. Terashima, and H. Suzuki. Turbulence structure and turbulence kinetic energy transport in multiscale/fractal-generated turbulence. *Phys. Fluids*, 25(6):065102, 2013.
  - [16] M. Obligado, T. Dairay, and J.C. Vassilicos. Nonequilibrium scalings of turbulent wakes. *Phys. Rev. Fluids*, 1:044409, 2016.
  - [17] J. Nedić, J.C. Vassilicos, and B. Ganapathisubramani. Axisymmetric turbulent wakes with new nonequilibrium similarity scalings. *Phys. Rev. Lett.*, 111(14):144503, 2013.
  - [18] T. Dairay, M. Obligado, and J.C. Vassilicos. Nonequilibrium scaling laws in axisymmetric turbulent wakes. *J. Fluid Mech.*, 781:166–195, 2015.
  - [19] S. Goto and J.C. Vassilicos. Energy dissipation and flux laws for unsteady turbulence. *Phys. Lett. A*, 379(16):1144–1148, 2015.
  - [20] A. Yoshizawa. Nonequilibrium effect of the turbulent-energy-production process on the inertial-range energy spectrum. *Phys. Rev. E*, 49(5):4065, 1994.
  - [21] S.L. Woodruff and R. Rubinstein. Multiple-scale perturbation analysis of slowly evolving turbulence. *J. Fluid Mech.*, 565:95, 2006.
  - [22] R. Rubinstein and T.T. Clark. Self-similar turbulence evolution and the dissipation rate transport equation. *Phys. Fluids*, 17(9):095104, 2005.
  - [23] K. Horiuti and T. Tamaki. Nonequilibrium energy spectrum in the subgrid-scale one-equation model in large-eddy simulation. *Phys. Fluids*, 25(12):125104, 2013.
  - [24] W. J. T. Bos, T.T. Clark, and R. Rubinstein. Small scale response and modeling of periodically forced turbulence. *Phys. Fluids*, 19:055107, 2007.

- [25] L.S.G. Kovaznay. Spectrum of locally isotropic turbulence. *J. Aeronaut. Sci.*, 15:745, 1948.
- [26] J.L. Lumley. Similarity and the turbulent energy spectrum. *Phys. Fluids*, 10:855, 1967.
- [27] S. Goto and J.C. Vassilicos. Local equilibrium hypothesis and Taylor's dissipation law. *Fluid Dyn. Res.*, 48(2):021402, 2016.
- [28] P.C. Valente, R. Onishi, and C.B. da Silva. Origin of the imbalance between energy cascade and dissipation in turbulence. *Phys. Rev. E*, 90(2):023003, 2014.
- [29] S. Goto and J.C. Vassilicos. Unsteady turbulence cascades *Phys. Rev. E* 94: 053108, 2016.